Investigation of time-based pressure control for microfluidics chip design

DOI : 10.36909/jer.14067

Sezgin Ersoy[*], Gurcan ATAKOK[**], Danial Khorsandi[***], Ersin Toptaş[*]

* Advanced Research in Mechatronics and Artificial Intelligence, Marmara University, Aydinevler Mah. Idealtepe Yolu No:15 34854 Maltepe/Istanbul/Turkey

** Department of Mechanical Engineering, Faculty of Technology, Marmara University, Aydinevler Mah. Idealtepe Yolu No:15 34854 Maltepe/Istanbul/Turkey

*** Procare Health, Department of medical affairs, 08860, Barcelona, Spain

Email: gatakok@marmara.edu.tr; **corresponding author

ABSTRACT

The emergence of the microfluidic chip was a game-changer in microbiological analysis platforms. This technology, by combining physics, chemistry, biology, and computing, helps researchers to obtain precise results in a shorter time. However, it requires more advancements in order to lessen its limitations. This study presents the design, modelling, and microbiological analysis of a microelectromechanical system (MEMS) based microfluidic chip. Three different microfluidic chips have been developed during the design process. These chips have different inlet channels and one outlet channel. The modelling process was carried out with Multiphysics Software. Pressure and velocity data in micron-sized channels were checked for each system. The flow directions of the fluids in the inlet and outlet channels were observed according to the pressure change. As a result of the analysis, the highest velocity was found in the microfluidic chip with three inlet channels. In comparison, the highest pressure was measured in the microfluidic chip with four inlet channels. These values are 2.36 $x10^{-17}$ m/s and 13.5 Pa, respectively. The pressure values of the 4 and 5-channel microfluidic chips were very close. The results showed that as the number of inlet channels increased, the pressure value in the microfluidic chip increased, but the velocity value decreased.

Keywords: Microfluidics, MEMS, Chip Design, Microprocessing

INTRODUCTION

The developments in the field of semiconductor technology has triggered a gradual increase in the study in field (Liu et al.,2018). With these studies, the foundations of today's microelectromechanical systems (MEMS) were laid by using different fabrication methods. These systems include devices designed and fabricated at micro and nano levels (Solouk et al.,2019). The design and fabrication process of microfluidics is also based entirely on MEMS technology. Many related words have emerged as the name of the modern research field that deals with microscopic length scales of transport routes and liquid-based devices, such as "MEMS- fluids" or "Bio-MEMS" and "microfluidics" (El Alami et al.,2019 & Onishi et al., 2017). MEMS fabrication (Rius et al.,2017) and actuation techniques (Algamili et al.,2021 & Tiwary et al.,2021) are seen in many application areas, including (Khorsandi et al.,2021) microfluidics, microactuator, biomedical (Mohd Ghazali et al.,2020), automotive (Bhatt et al.,2019), micro-robotics (Bucˇinskas et al.,2021 & Ghosh et al.,2021), wearable devices (Yang et al.,2021 & Cao et al.,2021), and microsensors (Unalli et al.,2020 & Waqar et al.,2021). In addition, different biomaterials, such as cells, organoids, and microorganisms, have been used in a variety of microfluidic chip applications (Tian et al.,2019 & Wang et al.,2021). Improvement in the integrated circuits and MEMS technology has been driven toward low cost, microfabrication, high density, and rapid operation speed (Pattanaik et al.,2021). The use of microfabrication methods to create microfluidic chips (Niculescu et al.,2021) and biosensors has facilitated biomedical research in many areas (Dalili et al.,2019 & Pranzo et al.,2018). Microfluidic chips are a technology designed at micro levels by combining fluid mechanics, physics, nanotechnology, and channels through which electric current can pass (Whitesides et al.,2006). In addition, microfluidics is the precise control and manipulation of liquids located in small, usually 10-100 μm channels, where the surface tension of the liquid flow and laminar effects are dominant. Here the fluid is defined as a group of channels or an integrated circuit in which air or heat passes through microfluidic channels ranging from a few μm to a few nm (Amin et al.,2016 & Ahrberg et al.,2016). Microfluidic devices can be made of polymers and glass to deliver and transport precise amounts of liquid to a sensing device. The most important application area of microfluidic chips is lab-on-a-chip (LOC) technology. The emergence of the LOC field on a chip has been realized with these chips. The microfluidics used in LOC devices are capable of producing millions of microchannels, each measuring just micrometers, on a single chip that can fit in hand (Chiriacò et al.,2018 & Khalid et al.,2017). Microchannels enable handling liquids as low as a few picolitres and manipulate biochemical reactions in minimal volumes. Microfluidic chips are also used more efficiently in many areas such as biomedical (Mahhengam et al.,2021), food (Schroen et al.,2021), chemistry (Theberge et al.,2012 & Schneider et al.,2021), medicine, pharmacy, and agriculture (Luecha et al.,2011) when they are well designed,

and structural analysis is done correctly (Huang et al. ,2019 & Li et al.,2018). In many designs, the chip takes up most of the workspace (Zhou et al.,2021).

Due to the variety of applications, optimization of a microfluidic chip becomes a crucial part of its design (Afzal et al.,2021). Recently, analysis of the pressure and velocity of the fluid flowing through the micron channels in the structure of the microfluidic system has gained significant importance (Sanjy et al.,2021). A MEMS-based microfluidic chip is presented in this study along with the modelling and microbiological analysis of the developed device fed with micro-litre liquid. In the modelling process, microfluidic systems with three different inlet channels (three, four, and five) and a single outlet channel have been developed. Pressure and velocity data in micron-sized channels were calculated for each system. At the same time, the flow directions of the fluids in the inlet and outlet channels were observed according to the change in pressure. Modelling and analysis processes were done using the analysis program. Utilizing the channels of the microfluidic chip, it will be possible to examine a chemical system and flow cell in the progression of the fluid or blood used in microbiological analysis processes.

METHODS

In this study, three different microfluidic chips with 3, 4, and 5 inlet channels and single outlet channel were designed. Micron-sized channels were created during the design process stage using 3D modeling software. After modeling, optimization of infusion pressure, micro-channel design, and time control are discussed. Increasing microchannels; It can increase sensitivity by performing different chemical reactions in parallel channels. The design process was carried out in two stages. First, a microfluidic design with 3, 4, and 5 inlet channels and a single outlet have been made. Later, as the comparison of three different microfluidics will depend on time, an appropriate 3D geometric design has been completed. The 3D designs and scaling of the 3, 4, and 5-channel microfluidic chip are shown in Figure 1. Each channel has a width of 30x30 μm and the channels which are located close to each other are determined as inlet channels. The inputs from these channels are collected in one channel and the outlet channel emerges. Recent advancements in the field of electronics resulted in the miniaturization of devices and circuits. This has allowed nano and micro level transmitters, be it active or passive, to be included in the microfluidic devices. The device presented in this paper can transmit data wirelessly using the surface acoustic wave-based communication technology.

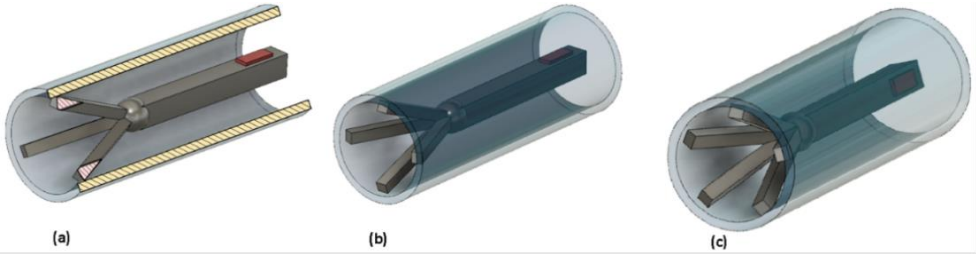

Figure 1 . 3D Models of microfluidic chips: a) 3 channels b) 4 channels c) 5 channels

MATHEMATICAL MODEL OF MICROFLUID CHIP

In this section, mathematical modeling of the microfluidic chip is described using the fluid model. The properties of saturated water determine this fluid model. Its dynamic viscosity is 0.001 Ns/m^2 and its density is 1000 kg/m^3. Before moving on to the mathematical model, the Reynolds number should be determined in order to find out whether the fluid is laminar or turbulent. This number is briefly the ratio of inertial forces to viscous forces and can be found using equation 1 as follows.

$$Re = \frac{puD}{\mu} = \frac{Inertial\ Forces}{Viscous\ Forces} \tag{1}$$

Here p (kg⁄m^3) is density, D (m) is the length of geometric characteristic, u (m/s) is flow rate. The length of the geometric characteristic varies according to the structure of the channel. D = 2ab / (a + b) for rectangular channels, D = a (side length) for square channels, and D = D (inner diameter) for circular channels. There are three different flows in liquid fluids flowing through the channels. These are laminar, transitive, and turbulent as follows, according to Reynold's number.

- Re < 2300 is considered as laminar flow.
- 2300 < Re < 4000 is transitional flow, that is, both flows can change randomly.
- Re > 4000 is considered as turbulent flow. (2)

Fluid dynamics can be found everywhere in daily life. Blood flowing in the body, especially in our body, water flowing from the faucet, and cool air blowing from the air conditioner are examples of these. When it comes to the fundamentals of fluid mechanics, which is based on the Newton's II law.

$$\sum \vec{f} = \vec{f}_{gravity} + \vec{f}_{pressure} + \vec{f}_{viscose} = \rho \frac{d\vec{u}}{dt} \tag{3}$$

Here, forces are values per unit volume; gravitational force, compression force, and viscous force, u is the fluid velocity, and ρ is density. Gravity is calculated as below:

$$f_{gravity} = \rho g \tag{4}$$

The force of gravity is given in Eq. (3). However, this situation is ignored since there is no flow through the microfluidic channel in any force direction opposite to the gravitational force. The developed model is used only for liquid flow with an enormous velocity showing laminar behavior. This means that with enough elements, we can get a numerical solution of the entire momentum balance and continuity equations for incompressible flow. The equations we need to solve are the Navier-Stokes equations in the time domain.

$$\rho \frac{\partial u}{\partial t} - pu\nabla u + \nabla p - \mu \nabla^2 \vec{V} = 0 \tag{5}$$

$$\frac{\partial u}{\partial x} + \frac{\partial v}{\partial y} + \frac{\partial w}{\partial z} = 0 \tag{6}$$

Here ρ denotes density (kg/m3), u is the velocity (m/s), μ is dynamic viscosity (Pa s), and p is pressure (Pa). In this case, the liquid is water with corresponding density and viscosity values. Since there is no electric field inside the fluid channel and the effect of hydrostatic pressure, the forces inside the channel are ignored.

$$\mu \nabla^2 \vec{V} = 0 \tag{7}$$

$$p = p_i \tag{8}$$

Due to the operations performed at micro levels, the counterforce of the viscosity in Eq. (6) was ignored. Therefore, the time-dependent equation of pressure is as follows.

$$p_i = 50 + 10\sin(\pi t + \alpha) \tag{9}$$

In this study, 'α' values for 3, 4, and 5 microfluidic channel chips designed are given in Table 1, respectively.

Table 1. 'α' value of microfluidic chips

Number of Inlet Channels	α Values (°)				
	Inlet 1	Inlet 2	Inlet 3	Inlet 4	Inlet 5
3-channel	α = 0	α = π/2	α = π		
4-channel	α = 0	α = π/4	α = 3π/4	α = π	
5-channel	α = 0	α = π/4	α = π/2	α = 3π/4	α = π

Time (t) values will be evaluated in the range of '0-4 s'. Also, liquid flows such as water and aqueous solutions are assumed to be incompressible in microfluidic channels, i.e., constant density ρ. Here the outlet channel is set to '0'. For all other limits, friction forces are not included in the x, y, and z axes.

MICROFLUIDIC CHIP ANALYSIS

In this study, the flow-velocity relationship of 3 different microfluidics designed in the upper part was established using the finite element method (FEM). In the obtained results, it was seen that as the number of channels increases, the flow rate decreases and accordingly the pressure value is higher. The flow analysis for each channel seen in Figure 2.

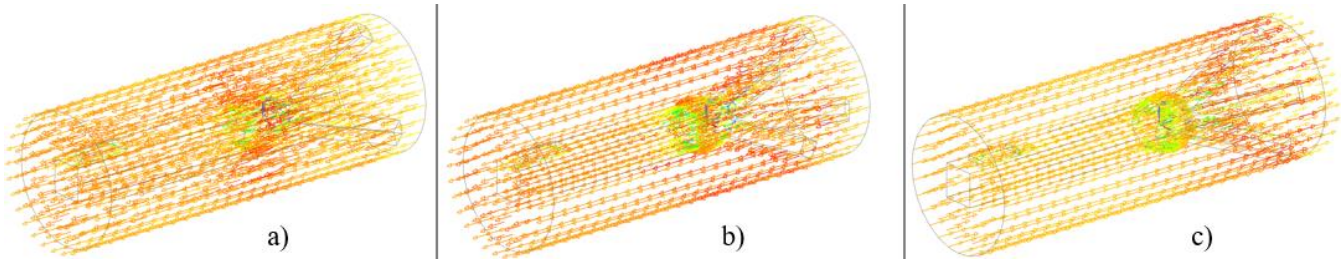

Figure 2. Each channels flow analysis: a) 3 channels b) 4 channels c) 5 channels

This relationship has been evaluated with the Multiphysics program using the MEMS toolbox. Using the Multiphysics program; It is possible to perform tests and analysis that are needed to be applied first by entering the parameters that are required to be tested in the program, either in the direction of a chip where microfluidic channels are created in 3D drawing programs or by drawing 3D or 2D microflow channels in the program. These analyses can give us the results which can help us in modifying the designs inline with the desired results before producing the sensor or chip. In addition, it will be possible to physically compare the tests required for the designed microfluidic environment in a virtual environment, and it will enable us to examine the channels for capillaries or fluids in different materials depending on time. The transfer of microfluidic chips to software and the modelling process are carried out in three stages. These stages are as follows, respectively.

- After the program was started, 'Laminar Flow' was selected as the fluid type. Pressure and velocity parameters and directions related to laminar flow are entered. In addition, the properties of the laminar fluid must be defined. Among these properties, density and dynamic viscosity have been entered as 1000 kg/m^3 and 0.001 Pa s, respectively.

- After the fluid type was determined, the microfluidic chips, whose solid model was created before, were transferred to the program.

- Then, the meshing process was applied following the flow dynamics according to each microfluidic flow dynamics (Figure 2). After the mesh slicing process is completed, the inlet parameters to be used for the microfluidic must be defined. In this section, it is necessary to enter the parameters in the program, define them together with the inlet and outlet positions for the "Inlet-Outlet" channel.

CONCLUSION

Since the 2000s, studies on microfluidic chips have increased using tissue and organ models to develop drugs. Microfluidic devices have been used in disease modelling, tissue development, and many other applications. A summary of these examples is shown in Figure 3.

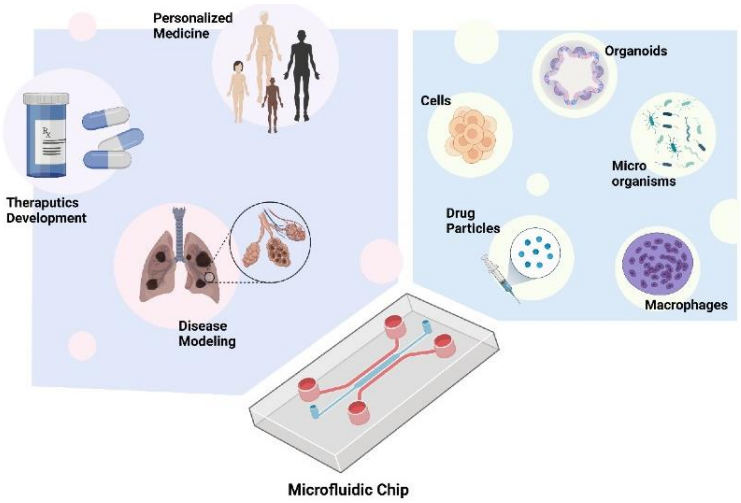

Figure 3 . Some examples of applications and biomaterials used in microfluidic chips designed for microbiological analysis

With these models, an organ on a chip has been developed by investigating biological processes (McLean et al.,2018 & Van der Helm et al.,2016). In the last decades, various types of microfluidic chips have emerged as a research platform for microbiologic analysis (Páez-Avilés et al.,2016 & Cui et al.,2019). Bilican et al. made a microbiological analysis of a pathogenic bacterium found in freshwater resources that poses a public health risk (Bilican et al.,2020). Here, a system for rapid analysis of spring water with a simple mechanism is proposed. The test, which takes 1h to complete, electrically interrogates the particles through a microfluidic chip suspended in the water sample. Kaminski et al. present microfluidic droplet applications in various fields of microbiology: i) detection and identification of pathogens, ii) antibiotic susceptibility testing, iii) microbial physiology studies, and iv) biotechnological selection and strain improvement (Kaminski et al.,2016). They also list challenges in the dynamically evolving field and potential new uses of droplets in microbiology. Grunberger et al. indicate a microfluidic single-cell cultivation platform that incorporates several hundred growth chambers, in which isogenic bacteria microcolonies growing in cell monolayers are tracked by automated time-lapse microscopy with spatiotemporal resolution (Gruenberger et al.,2013). The device was not explicitly improved for a specific organism but had a very generic configuration suitable for different microbial organisms. Wang et al. designed and fabricated a microfluidic chip to improve understanding of MICP at particle-scale by observing the behavior of bacteria and calcium carbonate crystals during the process (Wang et al.,2019). They found that bacteria became equally distributed throughout the microfluidic chip after the injection of bacterial suspension, grew along with bacterial settling, and detached during the injection of cementation solution. With these studies, up-to-date experimental studies are carried out for applications in food microbiology with LOC technology, isolation of plasma from whole blood using planar micro filters for laboratory applications on chips, and clogging of "T" connections on microfluidics

over time (Tsao et al.,2016 & Im et al.,2018 & Brassard et al.,2019). With the design and modelling process's completion, time-dependent pressure analyses were performed using the FEM. As explained in the previous section, firstly, the pressure parameters required for the boundary conditions of the microfluidic chips are entered, and dynamic viscosity and density are defined for the fluid information. Finally, the meshing process has been done. Likewise, FEM analysis started with the determination of the inlets and outlets of the microfluidic chip. This section will discuss the velocity and pressure analysis results by showing the 3, 4, and 5 microfluidic channel chip flow directions.

Table 2. Results depending on the experimental parameters.

		Inter Pressure Values [Pa]									Inlet α values				
		t=0	t=0.5	t=1	t=1.5	t=2	t=2.5	t=3	t=3.5	t=4	1	2	3	4	5
Ch. No.	Channel	3-channel microfluidic													
1	p_in_lm	50	40	50	60	50	40	50	60	50			π		
2	p_in_c	60	50	40	50	60	50	40	50	60		π/2			
3	p_in_rm	50	60	50	40	50	60	50	40	50	0				
Outlet pressure [Pa]		6.1	5.7	5.37	5.7	6.1	5.7	5.37	5.7	6.1					
Ch. No.	Channel	4-channel microfluidic													
1	p_in_lm	50	40	50	60	50	40	50	60	50				π	
2	p_in_il	57.7	42.9	42.9	57.7	57.7	42.9	42.9	57.7	57.7			3π/4		
3	p_in_ir	60	50	40	50	60	50	40	50	60		π/4			
4	p_in_rm	50	60	50	40	50	60	50	40	50	0				
Outlet pressure [Pa]		13.5	13	11.8	12.6	14	12.6	11.8	12.6	13.5					
Ch. No.	Channel	5-channel microfluidic													
1	p_in_lm	50	40	50	60	50	40	50	60	50					π
2	p_in_il	57.7	42.9	42.9	57.7	57.7	42.9	42.9	57.7	57.7				3π/4	
3	p_in_c	60	50	40	50	60	50	40	50	60			π/2		
4	p_in_ir	57.7	42.9	42.9	57.7	57.7	42.9	42.9	57.7	57.7		π/4			
5	p_in_rm	50	60	50	40	50	60	50	40	50	0				
Outlet pressure [Pa]		13	12	10.6	11.8	13	11.8	10.6	11.8	13					

These analyses were carried out in steps of 0.5 seconds with t = 0 - 4 seconds depending on the time. Results of experiments are given in Table 2 where all parameters are $10\sin(\pi t+\alpha)+50$.

$$10\sin(\pi t + \alpha) + 50 \tag{10}$$

THREE-CHANNEL MICROFLUIDIC CHIP ANALYSIS

Flow directions and data in 3-channel microfluidic at t = 0 s. When the color distribution depending on the pressure in the channel was examined, the flow should not change direction because the pressure values coming from channels 1 and 3 are equal. Flow directions and data in the 3-channel microfluidic chip at t=0.5s. When the color distribution depending on the pressure in the channel is examined, the pressure value coming from the number 1 channel is smaller than the pressure values from the other channels 2 and 3, so the flow had to change direction. Flow directions and data in the 3-channel microfluidic chip at t = 1 s. The pressure value coming from channels 1 and 3 is higher than the pressure values from the number 2 channels. However, due to the design of the microfluidic fluid, the inlets 1 and 3 balanced the pressure values to each other and

allowed the flow to continue through channel number 2. Flow directions and data in the 3-channel microfluidic chip at t=1.5 s. The pressure value coming from channels 1 and 2 is higher than the pressure values from the number 3 channels. In addition, since the pressure in the outlet channel is high, the pressure coming from the number 3 was insufficient, and the flow direction was reversed. There is a situation similar to t = 0.5 s. Flow directions and data in the 3-channel microfluidic chip at t=2 s. The pressure value coming from channels 1 and 3 is lower than the pressure values from the number 2 channels. The pressures of the fluids coming from the inlet number 1 and 3 balance each other; this situation caused the flow to flow more intensely through channel number 2. Flow directions and data in the 3-channel microfluidic chip at t=2.5 s. The pressure value coming from the 2 and 3 numbered channels is higher than the pressure values from the number 1 channel. Primarily, it caused the fluids encountered at the outlet to change direction. Here is a situation similar to the t=0.5 s case. Since the pressure coming from channel number 3 is higher than the others, the most flow from this channel was provided. Flow directions and data in the 3-channel microfluidic chip at t=3 s. The pressure value coming from channels 1 and 3 is higher than the pressure values from the number 2 channels. However, the pressures of the fluids coming from the inlet number 1 and 3 balance each other, and the fluid coming from channel number 2 slowed down, but the flow continued through this channel due to the channel design. If we compare the results from this graph to others, it is similar to the time t = 1 s. Flow directions and data in a 3-channel microfluidic chip at t=3.5 s. The pressure value coming from channels 1 and 2 is higher than the pressure values from the number 2 channels. The pressure coming from the number 1 channel is higher than the others caused the flow of the most flow from this channel due to the pressure difference. It also directed the flow direction from channel number 3 in the opposite way to normal. At the same time, it directed the fluid flowing from channel number 2 to some extent. Flow directions and data in a 3-channel microfluidic chip at t=4 s. Pressure values from channels 1 and 3 are lower than those from channel number 2. The pressure coming from channel number 2 was higher than the others, caused the flow of the most flow from this channel due to the pressure difference.

FOUR-CHANNEL MICROFLUIDIC CHIP ANALYSIS

Flow directions and data in the 4-channel microfluidic chip at t = 0 s. The pressure values coming from channels 1 and 4 are opposite to each other but of the same magnitude. On the other hand, the pressure values coming from the inlet numbers 2 and 3 are almost identical. Since the magnitude and direction of the pressure coming from the 2 and 3 channels are more significant and located in the direction closest to the exit direction, most of the flow is provided through these two channels. Flow directions and data in the 4-channel microfluidic chip at t = 0.5 s. The magnitudes of the pressures from channels 3 and 4 are more significant

than the pressure values from the other inlets 1 and 2. Due to the pressure difference between 4 and 1, the direction of the flow from inlet number 1 changes. At the same time, as the pressure value from number 2 is small, like number 1, it returns through the throat before the fluid comes to the outlet. Flow directions and data in the 4-channel microfluidic chip at t = 1 s. The fluid pressures coming from the inlet number 1 and 4 are equal to each other, and the highest pressure occurs in these two channels. However, this opposite equivalent size balances each other. Here, the fluids coming through channels 2 and 3 direct the fluids from 1 and 4 and drag them to the outlet. Flow directions and data in the 4-channel microfluidic chip at t = 1.5 s. When viewed from channel number 1 towards channel number 4, it is seen that the pressure decreases. In this case, since the pressure value of the fluid flowing through channels 1 and 2 is high, the size of the fluid flowing through channels 3 and 4 is too small to pass through the outlet channel, so it could not resist the pressure value coming from the other inlet channels and moves against the inlet direction. Flow directions and data in the 4-channel microfluidic chip at t = 2 s. The fluid pressures coming from the inlet number 1 and 4 are equal to each other, but the highest pressure occurs in the channel number 2 and 3. However, this opposite equal size balances each other. Here, the fluids coming through channels 2 and 3 direct the fluids from 1 and 4 and drag them to the outlet. Flow directions and data in the 4-channel microfluidic chip at t = 2.5 s. The magnitudes of the pressures coming from channels 3 and 4 are larger than the pressure values from the other inlets 1 and 2. Due to the pressure difference between 4 and 1, the direction of the flow from inlet number 1 changes. At the same time, as the pressure value from number 2 is small, like number 1, it returns through the throat before the fluid comes to the outlet. Flow directions and data in the 4-channel microfluidic chip at t = 3 s. The fluid pressures coming from the inlet number 1 and 4 are equal to each other and the highest pressure occurs in these two channels. However, this opposite equal size balances each other. Here, the fluids coming through channels 2 and 3 direct the fluids from 1 and 4 and drag them to the outlet. Flow directions and data in the 4-channel microfluidic chip at t = 3.5 s. When viewed from channel number 1 towards channel number 4, it is seen that the pressure decreases. In this case, since the pressure value of the fluid flowing through channels 1 and 2 is high, the size of the fluid flowing through channels 3 and 4 is too small to pass through the outlet channel, so it could not resist the pressure value coming from the other inlet channels and moves against the inlet direction. Flow directions and data in the 4-channel microfluidic chip at t = 4 s. The fluid pressures coming from the inlet number 1 and 4 are equal to each other, but the highest pressure occurs in the channel number 2 and 3. However, this opposite equal size balances each other. Here, the fluids coming through channels 2 and 3 direct the fluids from 1 and 4 and drag them to the outlet.

FIVE-CHANNEL MICROFLUIDIC CHIP ANALYSIS

Flow directions and data in the 5-channel microfluidic chip at t = 0 s. The pressure values coming from channels 1 and 4 are opposite to each other but of the same magnitude. On the other hand, the pressure values coming from inlets numbers 2, 3, and 4 are almost identical. Since the magnitude and direction of the pressure coming from the 2, 3, and 4 channels are more prominent and located in the direction closest to the exit direction, most of the flow is provided by the fluid in these channels. Flow directions and data in the 5-channel microfluidic chip at t = 0.5 s. The magnitudes of the pressures coming from channels 3, 4, and 5 are larger than the pressure values coming from the other inlets 1 and 2. Due to the pressure difference between 5 and 1, the direction of the flow from inlet number 1 changes. At the same time, as the pressure value from number 2 is small, like number 1, it returns through the throat before fluid comes to the outlet. Flow directions and data in the 5-channel microfluidic chip at t = 1 s. The fluid pressures coming from the inlet number 1 and 5 are equal, and the highest pressure occurs in these two channels. However, this opposite equal size balances each other. Here, the fluids coming from channels 2 and 4 direct some of the fluids from 1 and 5 and drag them to the outlet. The other part moves in the opposite direction to the flow direction due to the small pressure size in channel number 3. Flow directions and data in the 5-channel microfluidic chip at t = 1.5 s. When viewed from channel number 1 towards channel number 5, it is seen that the pressure decreases. In this case, since the pressure value of the fluid flowing through channels 1 and 2 is high, the size of the fluid flowing through channels 3 and 4 is too small to pass through the outlet channel, so it could not resist the pressure value coming from other inlet channels and moves opposite to the inlet direction. Flow directions and data in the 5-channel microfluidic chip at t = 2 s. Pressure sizes coming from channels 1 and 5 are opposite and equal. The most significant pressure is through channel number 3 and the most intense pressure flow towards the outlet. In this case, the flow from 1 and 5 is less. Flow directions and data in the 5-channel microfluidic chip at t = 2.5 s. When the pressure value is above 50 Pa at inlets number 3, 4, and 5, the flow flows steadily. However, when the pressure is as in channels 1 and 2 under 50 Pa, the flow direction is opposite to normal. Flow directions and data in the 5-channel microfluidic chip at t = 3 s are given in figure 4. The pressure value dropped only at inlet number 3 at 40 Pa. The pressure difference in this channel has changed the flow direction of the fluid coming from channel 3. Flow directions and data in the 5-channel microfluidic chip at t = 3.5. When the pressure differences in the channel are compared, it is at the lowest in inlets numbers 4 and 5. Therefore, the flow had to change its direction, since there is enough opposite size to affect the direction of the flow. Flow directions and data in the 5-channel microfluidic chip at t = 4 s. Except for the pressure value from number 3, flow values from other channels are close to each other. Since the flow from number 3 is directly in the same direction as the outlet, the most fluid going to the outlet goes from here.

PRESSURE-TIME ANALYSIS IN MICROFLUIDIC CHIP

In this section, pressure values occurring during the flow of microfluidic chips with 3, 4, and 5 inlet channels were measured depending on time. These values are taken from a point inside the outlet channel. The pressure-time graph of the fluid passing through the outlet channel of the 3-channel microfluidic chip is shown in figure 4. Here it is possible to divide the graph by dividing it into two. Because as seen in the figure, the graphic started to repeat after a point. As seen in figure 4, the pressure-time graph is similar in time intervals t = 0-1s and t = 2-3 s. Likewise, between t = 1-2 s and t = 3-4 s, the pressure in the channel increases and decreases at the same magnitude over time. If we take t = 0-1 s and t = 2-3 s time interval as a basis; the pressure in the outlet channel fell from 6.10 Pa to 5.37 Pa. In the other period, 370 pressure values increased from 5.37 Pa to 6.10 Pa. As seen in Figure 4 , pressure-time reference values taken from a point in the 4-channel microfluidic chip outlet channel are given. As seen in the figure, the graphic repeats periodically after a point. Since t = 0-1 s and t = 2-3 s time intervals are similar, pressure values are 13.5 Pa the highest and 11.75 Pa lowest if interpreted simultaneously. In the time interval between t = 1-2 s and t = 3-4 s, pressure values start from 11.75 Pa and increase up to 13.5 Pa. Pressure-time values taken from the outlet channel of the 5-channel microfluidic chip design are shown in Figure 4. Here, the graph continues periodically as in other 3 and 4 channel microfluidics. The pressure value decreased from 13 Pa to 10.6 Pa in the time interval t = 0-1 s and t = 2-3 s. Pressure values increased from 10.6 Pa to 13 Pa between t = 1-2 s and t = 3-4 s. Pressure-time values of 3, 4, and 5 microfluidic channel chips are summarized in the table in Figure 4.

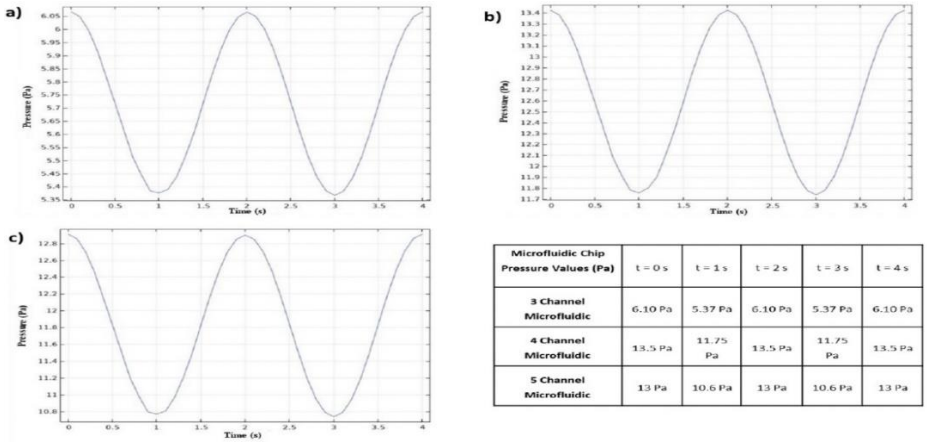

Microfluidic Chip Pressure Values (Pa)	t = 0 s	t = 1 s	t = 2 s	t = 3 s	t = 4 s
3 Channel Microfluidic	6.10 Pa	5.37 Pa	6.10 Pa	5.37 Pa	6.10 Pa
4 Channel Microfluidic	13.5 Pa	11.75 Pa	13.5 Pa	11.75 Pa	13.5 Pa
5 Channel Microfluidic	13 Pa	10.6 Pa	13 Pa	10.6 Pa	13 Pa

Figure 4. Microfluidic chip pressure-time graph and values. (a) 3-Channel microfluidic chip pressure-time graph, (b) 4-Channel microfluidic chip pressure-time graph, and (c) 5-Channel microfluidic chip pressure-time graph

VELOCITY-TIME ANALYSIS IN MICROFLUIDIC CHIP

In this section, velocity-time values of 3, 4, and 5 microfluidic channel chips are obtained. These values are measured over a reference point taken from the outlet channel. The velocity-time plot of a 3-channel microfluidic chip is shown in Figure 5. The graph includes the time interval t = 0-4 s, and as can be seen, it repeats itself periodically after a point. As seen in figure 5, the fluid velocity from the outlet channel decreased from $2.36x10^{-17}$ m/s to $2.1x10^{-17}$ m/s between t=0-1s and 2-3s. In the time interval t = 1-2 s and t=3-4 s, it accelerated from $2.1x10^{-17}$ m/s to $2.36x10^{-17}$ m/s. The values of the velocity-time graph measured from the outlet switch of the 4-channel microfluidic chip are given in Figure 5 . As seen in the figure, the graph shows the time interval t = 0-4 s, and the graph repeats periodically after t = 2 s. In the time interval from t = 0-1 s to t = 2-3 s, the velocity starts from $0.58x10^{-17}$ m/s and decreases to $0.51x10^{-17}$ m/s. In the time interval between t = 1-2 s and t = 3-4 s, the velocity started from $0.51x10^{-17}$ m/s and increased to $0.58x10^{-17}$ m/s. The values of the velocity-time graph from the outlet switch of the 5-channel microfluidic chip are given in Figure 5 . This graph contains data in the time interval t=0-4 s. The graph continuous periodically after a certain point. In the time interval t = 0-1 s and t = 2-3 s, the velocity starts from $1.54x10^{-17}$ m/s and decreases to $1.28x10^{-17}$ m/s. In the time interval t=1-2 s and t=3-4 s, the velocity decreases from $1.28x10^{-17}$ m/s to $1.54x10^{-17}$ m/s. Velocity-time values of 3, 4, and 5 microfluidic channel chips are summarized in the table in Figure 5.

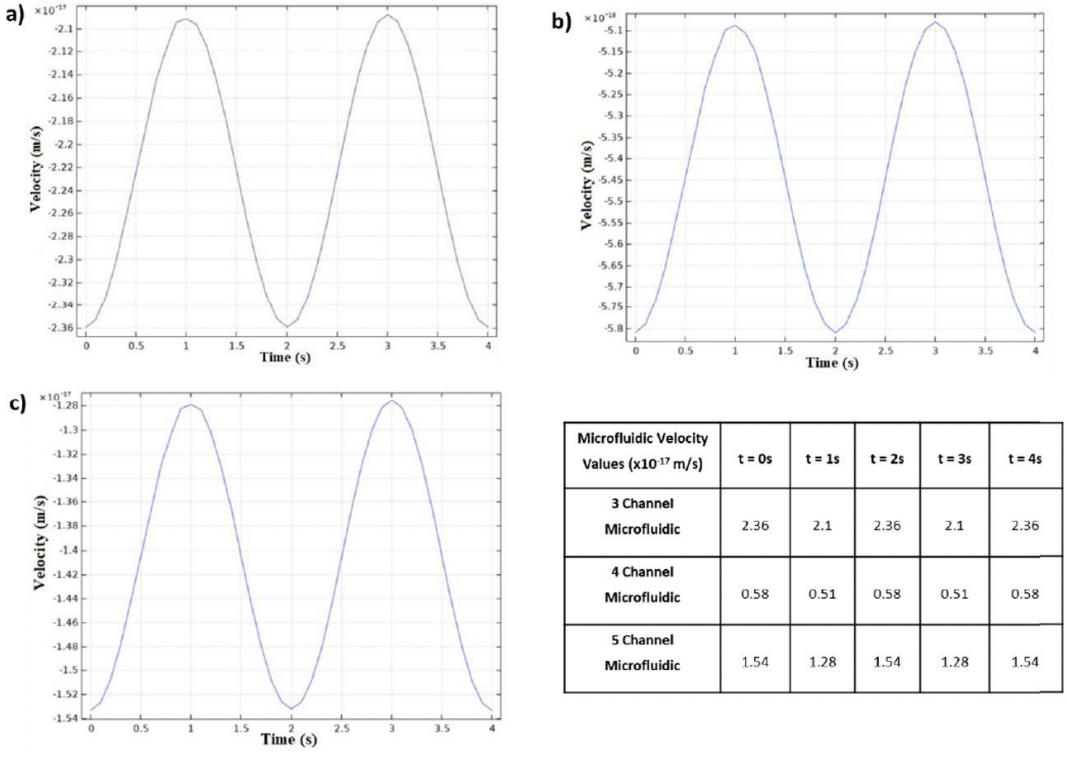

Microfluidic Velocity Values ($x10^{-17}$ m/s)	t = 0s	t = 1s	t = 2s	t = 3s	t = 4s
3 Channel Microfluidic	2.36	2.1	2.36	2.1	2.36
4 Channel Microfluidic	0.58	0.51	0.58	0.51	0.58
5 Channel Microfluidic	1.54	1.28	1.54	1.28	1.54

Figure 5. Microfluidic chip velocity-time graph and values. (a) 3-Channel microfluidic chip velocity-time graph, (b) 4-Channel microfluidic chip velocity-time graph, and (c) 5-Channel microfluidic chip velocity-time graph.

DISCUSSION

In this study, design, modelling, and microbiological analysis of MEMS-based microfluidic chip with 3, 4, and 5 inlet and single outlet channels using software. Microfluidics designed using solid modeling software were tested one by one by giving a fluid model in software. The same liquid fluid model is used for all microfluidic designs. In line with the analyzes, pressure and velocity data in micron-sized channels were checked for each system. Also, the flow directions of the fluids in the inlet and outlet channels were observed according to the change in pressure. The results of this study are seen here with the highest velocity of $2.36x10^{-17}$ m/s in line with the researches in the design of the 3-channel microfluidic chip. Considering the pressure in the 3-channel microfluidic chip, the lowest pressure is 5.37 Pa. The flow rate is the lowest in the microfluidic chip with 4 inlet channels. This value is $0.51x10^{-17}$ m/s. On the other hand, in the microfluidic chip with 4 channel inlets, the pressure is the highest, and this value is 13.5 Pa. Finally, the highest pressure was 13 Pa, and the highest velocity was $1.54x10^{-17}$ m/s in the 5-channel microfluidic chip. The results showed that as the number of inlet channels increased, the pressure value in the microfluidic chip increased, but the velocity value decreased. These microfluidic chips to be produced can be used to instantly control data such as pulse, blood flow, blood pressure from the human body and to transmit data such as location-location transmission to the required places, or can be used in a chemical process. Chemical reactors, heat exchangers, separators, and mixers performing microprocessing can also be used.

REFERENCES

Afzal, A. & Kim, K.-Y. ,2021 Analysis and Design Optimization of Micromixers. SpringerBriefs in Applied Sciences and Technology, Springer Singapore, Singapore.

Ahrberg, C. D., Manz, A. & Chung, B. G.2016 Polymerase chain reaction in microfluidic devices. Lab on a Chip 16, 3866–3884, DOI: 10.1039/C6LC00984K .

Algamili, A. S. et al. 2021 A Review of Actuation and Sensing Mechanisms in MEMS-Based Sensor Devices. Nanoscale Res. Lett. 16, 16, DOI: 10.1186/s11671-021-03481-7 .

Amin, R. et al. 2016 3D-printed microfluidic devices. Biofabrication 8, 22001, DOI: 10.1088/1758-5090/8/2/022001 .

Bhatt, G., Manoharan, K., Chauhan, P. S. & Bhattacharya, S. 2019 MEMS Sensors for Automotive Applications: A Review, 223–239 (Springer Singapore, Singapore,).

Bilican, I., Bahadir, T., Bilgin, K. & Guler, M. T. 2020 Alternative screening method for analyzing the water samples through an electrical microfluidics chip with classical microbiological assay comparison of P. aeruginosa. Talanta 219, 121293, DOI:10.1016/j.talanta.2020.121293 .

Brassard, D. et al. 2019 Extraction of nucleic acids from blood: unveiling the potential of active pneumatic pumping in centrifugal microfluidics for integration and automation of sample preparation processes. Lab on a Chip 19, 1941–1952, DOI: 10.1039/C9LC00276F .

Bučinskas, V., Subačiūtė-Žemaitienė, J., Dzedzickis, A. & Morkvėnaitė-Vilkončienė, I. 2021 Robotic micromanipulation: a) actuators and their application. Robotic Syst. Appl. 1, 2–23, DOI: 10.21595/rsa.2021.22071 .

Cao, Z., Wen, Q., Wang, X., Yang, Q. & Jiang, F. 2021 An Overview of the Miniaturization and Endurance for Wearable Devices. J. on Internet Things 3, 11–17, DOI: 10.32604/jiot.2021.010404 .

Chiriacò, M. et al. 2018 Lab-on-Chip for Exosomes and Microvesicles Detection and Characterization. Sensors 18, 3175, DOI:10.3390/s18103175 .

Cui, P. & Wang, S. 2019 Application of microfluidic chip technology in pharmaceutical analysis: A review. J. Pharm. Analysis 9, 238–247, DOI: 10.1016/j.jpha.2018.12.001 .

Dalili, A., Samiei, E. & Hoorfar, M. 2019 A review of sorting, separation and isolation of cells and microbeads for biomedical applications: microfluidic approaches. The Analyst 144, 87–113, DOI: 10.1039/C8AN01061G .

El Alami El Hassani, N. et al. 2019 Development and application of a novel electrochemical immunosensor for tetracycline screening in honey using a fully integrated electrochemical Bio-MEMS. Biosens. Bioelectron. 130, 330–337, DOI:10.1016/j.bios.2018.09.052 .

Ghosh, B., Jain, R. K., Majumder, S., Roy, S. S. & Mukhopadhyay, S. 2017 Experimental performance evaluation of smart bimorph piezoelectric actuator and its application in micro robotics. Microsyst. Technol. 23, 4619–4635, DOI:10.1007/s00542-017-3273-4 .

Gruenberger, A. et al. 2013 Microfluidic Picoliter Bioreactor for Microbial Single-cell Analysis: Fabrication, System Setup, and Operation. J. Vis. Exp. DOI: 10.3791/50560 .

Huang, Q., Mao, S., Khan, M. & Lin, J.-M. 2019 Single-cell assay on microfluidic devices. The Analyst 144, 808–823, DOI:10.1039/C8AN01079J .

Im, S. B., Uddin, M. J., Jin, G. J. & Shim, J. S. 2018 A disposable on-chip microvalve and pump for programmable microfluidics. Lab on a Chip 18, 1310–1319, DOI: 10.1039/C8LC00003D .

Kaminski, T. S., Scheler, O. & Garstecki, P. 2016 Droplet microfluidics for microbiology: techniques, applications and challenges. Lab on a Chip 16, 2168–2187, DOI: 10.1039/C6LC00367B .

Khalid, N., Kobayashi, I. & Nakajima, M. 2017 Recent lab-on-chip developments for novel drug discovery. Wiley Interdiscip. Rev. Syst. Biol. Medicine 9, e1381, DOI: 10.1002/wsbm.1381 .

Khorsandi, D. et al. 2021 Manufacturing of Microfluidic Sensors Utilizing 3D Printing Technologies: A Production System. J. Nanomater. 2021, DOI: https://doi.org/10.1155/2021/5537074 .

Li, W. et al. 2018 Microfluidic fabrication of microparticles for biomedical applications. Chem. Soc. Rev. 47, 5646–5683, DOI:10.1039/C7CS00263G .

Liu, H., Zhang, L., Li, K. & Tan, O. 2018 Microhotplates for Metal Oxide Semiconductor Gas Sensor Applications—Towards the CMOS-MEMS Monolithic Approach. Micromachines 9, 557, DOI: 10.3390/mi9110557 .

Luecha, J., Hsiao, A., Brodsky, S., Liu, G. L. & Kokini, J. L. 2011 Green microfluidic devices made of corn proteins. Lab on a Chip 11, 3419, DOI: 10.1039/c1lc20726a .

Mahhengam, N. et al. 2021 Applications of Microfluidic Devices in the Diagnosis and Treatment of Cancer: A Review Study. Critical Rev. Anal. Chem. 1–15, DOI: 10.1080/10408347.2021.1922870 .

McLean, I. C., Schwerdtfeger, L. A. 2018, Tobet, S. A. & Henry, C. S. Powering ex vivo tissue models in microfluidic systems. Lab on a Chip 18, 1399–1410, DOI: 10.1039/C8LC00241J .

Mohd Ghazali, F. A. et al. 2020 MEMS actuators for biomedical applications: a review. J. Micromechanics Microengineering 30, 73001, DOI: 10.1088/1361-6439/ab8832 .

Niculescu, A.-G., Chircov, C., Bîrcă, A. C. & Grumezescu, A. M. 2021 Fabrication and Applications of Microfluidic Devices: A Review. Int. J. Mol. Sci. 22, 2011, DOI: 10.3390/ijms22042011 .

Onishi, S. et al. 2017 (Invited) Detection of Bacterial Fluorescence by the Combination of MEMS Microfluidic Chip and Si Photodetector toward On-Chip Biological Sensing. ECS Transactions 80, 157–164, DOI: 10.1149/08004.0157ecst .

Páez-Avilés, C. et al. 2016 Combined Dielectrophoresis and Impedance Systems for Bacteria Analysis in Microfluidic On-Chip Platforms. Sensors 16, 1514, DOI: 10.3390/s16091514 .

Pattanaik, P. & Ojha, M. 2021 Review on challenges in MEMS technology. Mater. Today: Proc. DOI: 10.1016/j.matpr.2021.03. 142 .

Pranzo, D., Larizza, P., Filippini, D. & Percoco, G. 2018 Extrusion-Based 3D Printing of Microfluidic Devices for Chemical and Biomedical Applications: A Topical Review. Micromachines 9, 374, DOI: 10.3390/mi9080374 .

Rius, G., Baldi, A., Ziaie, B. & Atashbar, M. Z. 2017 Introduction to Micro-/Nanofabrication. 51–86, DOI: 10.1007/978-3-662-54357-3_3 .

Sanjy, A., Trellet, M., Nicolas, L., Clerget, C.-H. & Petit, N., 2021. No Title. In 11th IFAC International Symposium on Advanced Control of Chemical Processes (ADCHEM) .

Schneider, S., Gruner, D., Richter, A. & Loskill, P. 2021 Membrane integration into PDMS-free microfluidic platforms for organ-on-chip and analytical chemistry applications. Lab on a Chip 21, 1866–1885, DOI: 10.1039/D1LC00188D .

Schroen, K. et al. 2021 Droplet Microfluidics for Food and Nutrition Applications. Micromachines 12, 863, DOI: 10.3390/mi12080863.

Solouk, M. R., Shojaeefard, M. H. & Dahmardeh, M. 2019 Parametric topology optimization of a MEMS gyroscope for automotive applications. Mech. Syst. Signal Process. 128, 389–404, DOI: 10.1016/j.ymssp.2019.03.049 .

Theberge, A. B. et al. 2012 Microfluidic platform for combinatorial synthesis in picolitre droplets. Lab on a Chip 12, 1320–1326, DOI: 10.1039/C2LC21019C .

Tian, C., Tu, Q., Liu, W. & Wang, J. 2019 Recent advances in microfluidic technologies for organ-on-a-chip. TrAC Trends Anal. Chem. 117, 146–156, DOI: 10.1016/j.trac.2019.06.005 .

Tiwary, A. & Rout, S. S. 2021 MEMS Devices and Thin Film-Based Sensor Applications. In Lata Tripathi, S., Ahmad Alvi, P. & Subramaniam, U. (eds.) Electrical and Electronic Devices, Circuits and Materials, DOI: 10.1201/9781003097723 (CRC Press, First edition. | Boca Raton, FL : CRC Press/Taylor Francis,).

Tsao, C.-W. 2016 Polymer Microfluidics: Simple, Low-Cost Fabrication Process Bridging Academic Lab Research to Commer- cialized Production. Micromachines 7, 225, DOI: 10.3390/mi7120225 .

Unalli, I., Ersoy, S. & Ertugrul, I. 2020 Microfluidics chip design analysis and control. J. Mechatronics Artif. Intell. Eng. 1, 2–7, DOI: 10.21595/jmai.2020.21470 .

Van der Helm, M. W., van der Meer, A. D., Eijkel, J. C. T., van den Berg, A. & Segerink, L. I. 2016 Microfluidic organ-on-chip technology for blood-brain barrier research. Tissue Barriers 4, e1142493, DOI: 10.1080/21688370.2016.1142493 .

Wang, L. et al. 2021 Advances in reconstructing intestinal functionalities in vitro: From two/three dimensional-cell culture platforms to human intestine-on-a-chip. Talanta 226, 122097, DOI: 10.1016/j.talanta.2021.122097 .

Wang, Y., Soga, K., Dejong, J. T. & Kabla, A. J. 2019 A microfluidic chip and its use in characterising the particle-scale behaviour of microbial-induced calcium carbonate precipitation (MICP). G@ACUTEACCENT@eotechnique 69, 1086–1094, DOI:10.1680/jgeot.18.P.031.

Waqar, T. & Ersoy, S. 2021 Design and Analysis Comparison of Surface Acoustic Wave-Based Sensors for Fabrication Using Additive Manufacturing. J. Nanomater. 2021, 1–12, DOI: 10.1155/2021/5598347 .

Whitesides, G. M. 2006 The origins and the future of microfluidics. Nature 442, 368–373, DOI: 10.1038/nature05058 .

Yang, X. & Zhang, M. 2021 Review of flexible microelectromechanical system sensors and devices. Nanotechnol. Precis. Eng. 4, 025001, DOI: 10.1063/10.0004301 .

Zhou, Z., Zhang, W., Yuan, H., Jiang, Q., Wang, Y., Jin, X., Peng, Y. & Luo, J. 2021 An On-Chip TVS Design to Meet System Level ESD Protection For RS485 Transceiver. Journal of Engineering Research Vol.10 No. (1b) 252-263, DOI: 10.36909/Jer.9715